Optimal Surface Roughness of an Implant to Generate Osseointegration and Biological Fixation

Carlos A. Vega,[*] Favio Moruno,[**] Diego Veneri[**]

[*]Orthopedics and Traumatology Service, Hospital Central de San Isidro "Dr. Melchor Ángel Posse", San Isidro, Buenos Aires, Argentina.
[**]Orthopedics and Traumatology Service, Hospital Zonal General de Agudos "Dr. Carlos Bocalandro", Tres de Febrero, Buenos Aires, Argentina.

ABSTRACT

Introduction: The use of rough surfaces for biological fixation in implants is an increasingly common alternative. The aim of this study is to determine the optimal surface roughness of an intramedullary implant to promote osseointegration and subsequent biological fixation, using thermal arc projection and rabbit femurs as a biological receptor model. **Materials and Methods:** Cylindrical intramedullary systems with rough titanium coatings were implanted with varying degrees of roughness to assess where optimal osseointegration occurs, using the femurs of six rabbits (unilateral). The osseointegration process was monitored through monthly radiographs and histopathological analysis of the femur specimens. **Results:** No migration or subsidence occurred in any of the implants. Radiographic evidence of osseointegration was observed in all femurs. Bone formation was established around all implants. However, a mechanical test to evaluate the strength of the adhesion to the bone could not be performed. **Conclusion:** Surfaces with a roughness >100 µm have shown a favorable biological response, demonstrating a direct bond between the implant surface and the bone.

Keywords: Roughness; osseointegration; titanium; thermal projection.

Rugosidad óptima de un implante para generar la osteointegración y la fijación biológica

RESUMEN

Introducción: El uso de superficies rugosas para la fijación biológica en implantes es una alternativa que se está usando cada vez con más frecuencia. El objetivo del estudio fue determinar la rugosidad óptima de un implante endomedular que permita la osteointegración y la consecuente fijación biológica, mediante la proyección térmica por arco utilizando fémures de conejos como modelo biológico receptor. **Materiales y Métodos:** Se implantaron sistemas endomedulares cilíndricos con recubrimiento rugoso de titanio y distinto rango de rugosidad en fémures de seis conejos (unilaterales) para determinar dónde se produce una mayor osteointegración. El proceso de osteointegración se evaluó con radiografías mensuales y estudios de anatomía patológica del fémur del espécimen. **Resultados:** No se produjo migración o subsidencia en ninguno de los implantes. Todos los fémures mostraron signos de osteointegración radiográfica. Se demostró la presencia de neoformación ósea establecida alrededor de todos los implantes. Sin embargo, no se pudo realizar un testeo mecánico para evaluar la fuerza de adhesión al hueso. **Conclusión:** Las superficies con rugosidades >100 µm proporcionan una respuesta biológica favorable con una unión directa entre la superficie de los implantes y el hueso.

Palabras clave: Rugosidad; osteointegración; titanio; proyección térmica.

INTRODUCTION

The long-term success of total hip arthroplasty depends on stable anchorage to the bone. To achieve lasting stability with cementless implants, osseointegration is essential for establishing permanent fixation, i.e., proper attachment of lamellar bone to the implant without fibrous tissue interposition.[1,2] The success of biological fixation primarily depends on meticulous surgical techniques, the type of material used, and the primary stability of

Received on March 1st, 2024. Accepted after evaluation on August 8th, 2024 • Dr. CARLOS A. VEGA • c_vega78@hotmail.com https://orcid.org/0000-0002-6104-5099

How to cite this article: Vega CA, Moruno F, Veneri D. Optimal Surface Roughness of an Implant to Generate Osseointegration and Biological Fixation. *Rev Asoc Argent Ortop Traumatol* 2024;89(5):507-518. https://doi.org/10.15417/issn.1852-7434.2024.89.5.1930

the implant. The osseointegration process manifests as interdigitation within small pores (ingrowth) or through bone growth on a rough surface (ongrowth).[3,4] Research on osseointegration focuses on identifying suitable materials that promote this type of fixation. Various materials have been studied: from the Swedish school of Brånemark's introduction of dental implants with machined rough surfaces,[5] to the Swiss school of Schroeder's use of titanium plasma as an inert material, and hydroxyapatite as a bioactive material, to more recent innovations, such as tantalum rough surfaces, 3D printing of rough textures, and electron beam techniques. These developments are supported by a long history of intensive research, including laboratory (in vitro) and animal (in vivo) studies. [6,7]

To improve the quality of osseointegration, there has been an ongoing search for new elements, structures, and implant dimensions that can be used in demanding conditions to guarantee durability. The use of rough surfaces for biological fixation has become an increasingly common alternative. Recent research efforts have focused on identifying a rough material with an optimal structure to facilitate bone growth.[8] In all cases, the goal remains to achieve adequate osseointegration.

Experimental animal studies have demonstrated implant fixation through bone apposition and growth both on the surface and within porous systems. Current clinical reviews suggest radiological and histological evidence of bone growth in direct contact with the implant material and inside porous systems, thereby combining the bioactive properties of hydroxyapatite with the mechanical properties of metals, while avoiding the fragility issues of fully ceramic implants.[9] In modern total hip arthroplasty, femoral stems are typically made from various alloys, with titanium-aluminum-vanadium (Ti6Al4V, grade 5 titanium) being the preferred material for cementless femoral stems. This alloy offers several advantages over others, including superior biocompatibility, a low modulus of elasticity that closely resembles bone, and better load transmission (112,000 MPa), which supports favorable bone remodeling and enhances osseointegration. It also has relatively low toxicity at clinically encountered concentrations and is inert in physiological environments.[10,11] Furthermore, it allows bone to grow into its structure, providing robust biological fixation to the surrounding tissue. [12,13]

The aim of this study was to determine the optimal implant roughness and evaluate the intramedullary osseointegration process—resulting from biological fixation (secondary stabilization)—using implants created through thermal arc spraying. The study used rabbit femurs as a receptor model and investigated the bone-implant interface through radiographic and anatomical pathology analyses.

MATERIALS AND METHODS

Cylindrical intramedullary systems with rough titanium coatings were implanted in the femurs of six skeletally mature New Zealand rabbits, each weighing approximately 5 kg. Over a 12-week period, all surgical procedures were performed at Fundación Favaloro, where the project was presented to the Bioethics Committee and received approval.

For the characteristics mentioned, titanium-aluminum-vanadium alloy was chosen as the material, combined with a rough thermal spray coating. Thermal spraying is a process in which a metallic coating is applied through the deposition of molten particles, which are accelerated and sprayed at high pressure onto the surface of a base material or substrate. This process can be categorized into three main methods: flame spraying, arc spraying, and plasma spraying.

In this study, electric arc spraying was employed to generate the rough coating. This technique involves two titanium metal wires that serve as electrodes. When the wires come into contact, they create a short circuit that forms an electric arc,[14] causing the wires to melt and project as particles onto the previously shot-blasted substrate. The particles are spread depending on the system's compressed air, in an inert argon gas environment (Figure 1).

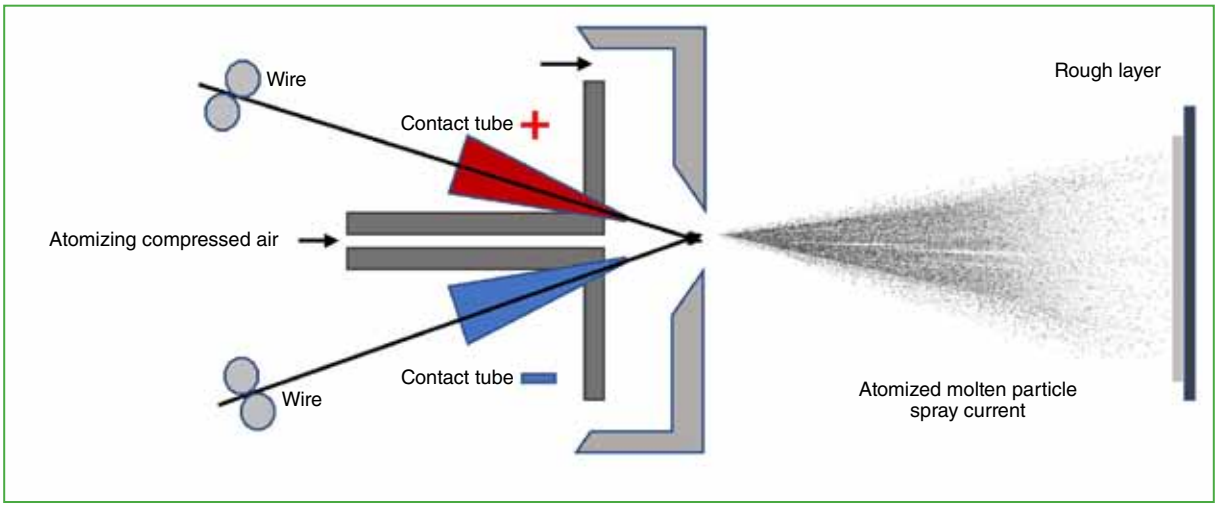

Figure 1. Schematic diagram of the electric arc spray system.

The resulting rough surface depends on the exposure time of the molten particles impacting the implant. Surface roughness was measured using a MITUTOYO model SJ 210 roughness meter (Figure 2), which quantifies the effective profile based on specific geometric characteristics. These measurements were corroborated by the National Institute of Industrial Technology and the School of Engineering of La Plata. The analysis included the distances between roughness peaks (Ra, the maximum distance between peaks over a baseline length) and the depth of roughness between peaks (Rt, the largest peak-to-valley distance across all baseline lengths) (Figure 3).

Figure 2. Mitutoyo surface roughness tester model SJ 210.

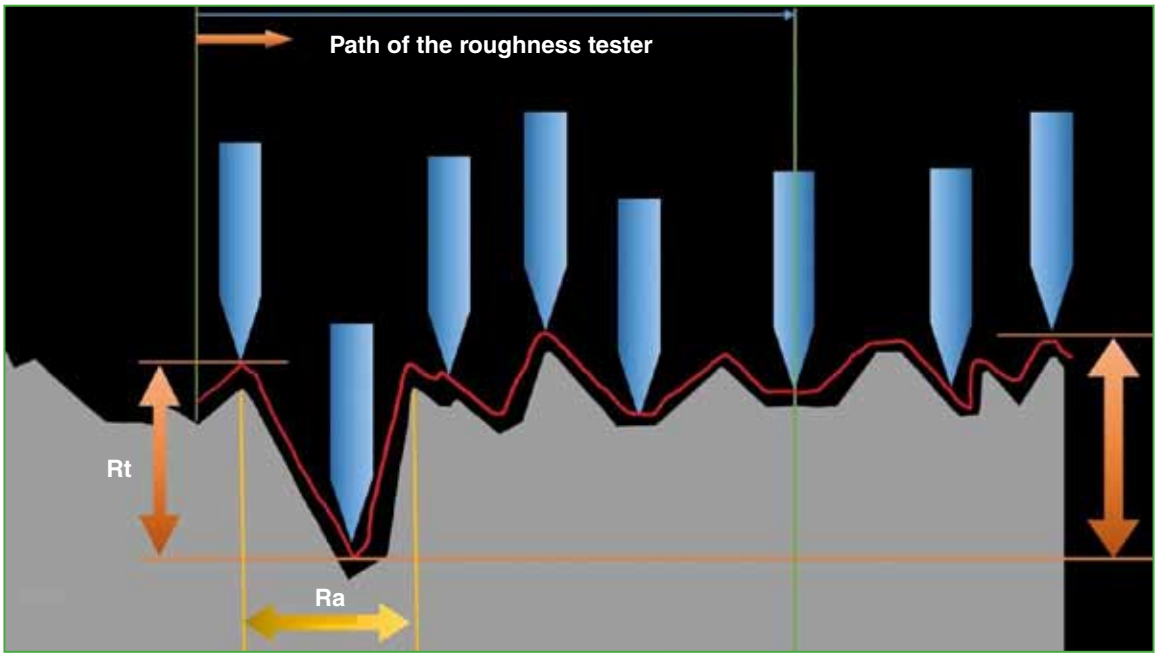

Figure 3. Path of the surface roughness tester for Ra and Rt measurement.
Ra = maximum peak-to-peak distance in a basic length; Rt = largest peak-to-valley distance of all basic lengths.

The intramedullary implants for the biological recipients were specifically designed for this study. Preoperative planning involved measuring the diameter of the proximal femur (metaphyseal-diaphyseal zones) of a prototype rabbit using full-size anteroposterior and lateral radiographs. As a result of this planning, titanium alloy implants with three diameters (3, 3.5, and 4 mm) and three lengths for each diameter (30, 35, and 40 mm) were created (Figure 4), providing a set of nine implants per rabbit (Figure 5).

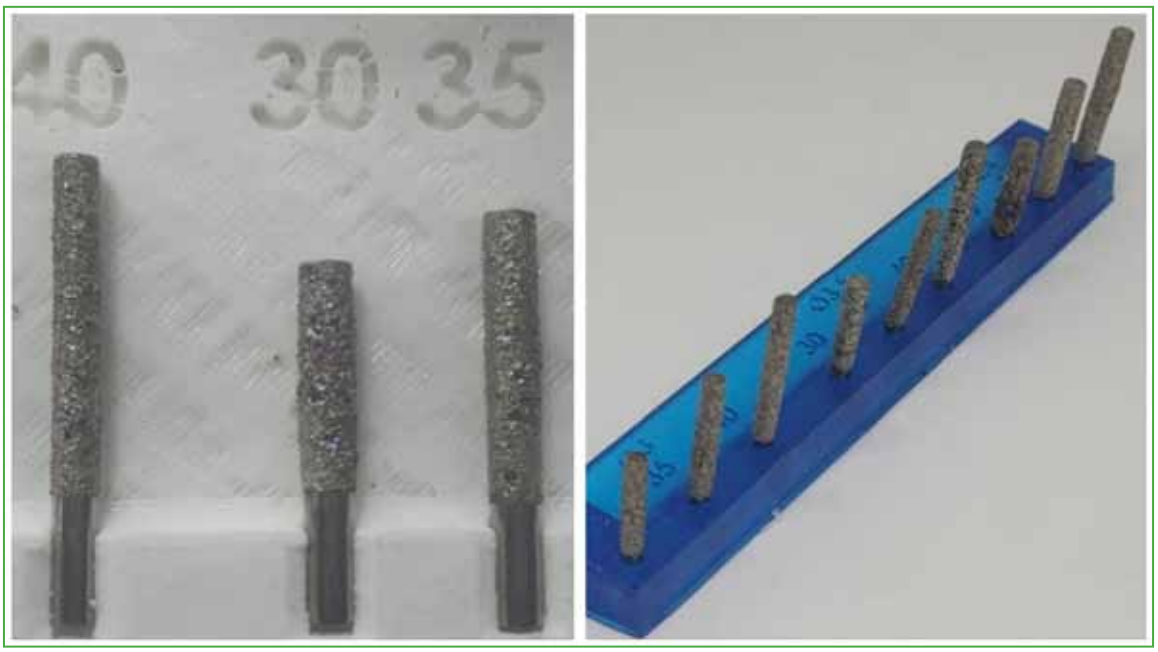

Figure 4. Titanium alloy implants used, with different lengths and diameters.

Figure 5. Individual placement set for each specimen.

To enhance precision, each stem was divided into two halves (anterior and posterior), marked to differentiate two surfaces. One half had an average roughness of 120 µm (range 100–150 µm), while the other half had a lower average roughness of 70 µm (range 30–90 µm). This division simplified the analysis of osseointegration in relation to roughness from an anatomical pathology perspective.

The osseointegration process was studied using monthly radiographs to identify union points according to Gruen's zone classification. At the end of the third month, an anatomical pathology study was conducted on the femurs. Each femur was individually fixed in 10% formaldehyde. The bones were then decalcified using Extra Decalcifier (Biopur Diagnostics, Biopur SRL, Rosario, Argentina) to extract bone fragments for study, preserving the bone-implant interface for subsequent eosin and hematoxylin staining. This analysis was performed using an optical microscope.

Radiographs were taken immediately postoperatively and again at 12 weeks after implantation to confirm proper implant placement and rule out fractures. Radiographs were also taken at the time of extraction to document successful implant incorporation (Figure 6). The rabbits were then euthanized, and femurs were collected from all animals. Radiographs of the extracted femurs were taken in anteroposterior and lateral projections, allowing analysis according to Gruen's zone classification to identify areas of bone growth (Figure 7).

During histological sampling, a macroscopic analysis was performed, revealing the growth of cancellous bone around the implants (Figure 8). A microscopic examination of the tissue surrounding the implants followed, with bone growth quantified based on the presence of mature bone and cortical osteogenesis in the intramedullary area.

At the time of euthanasia, after three months, all implants had satisfactorily osseointegrated.

Figure 6. Immediate postoperative radiographs of the specimens.

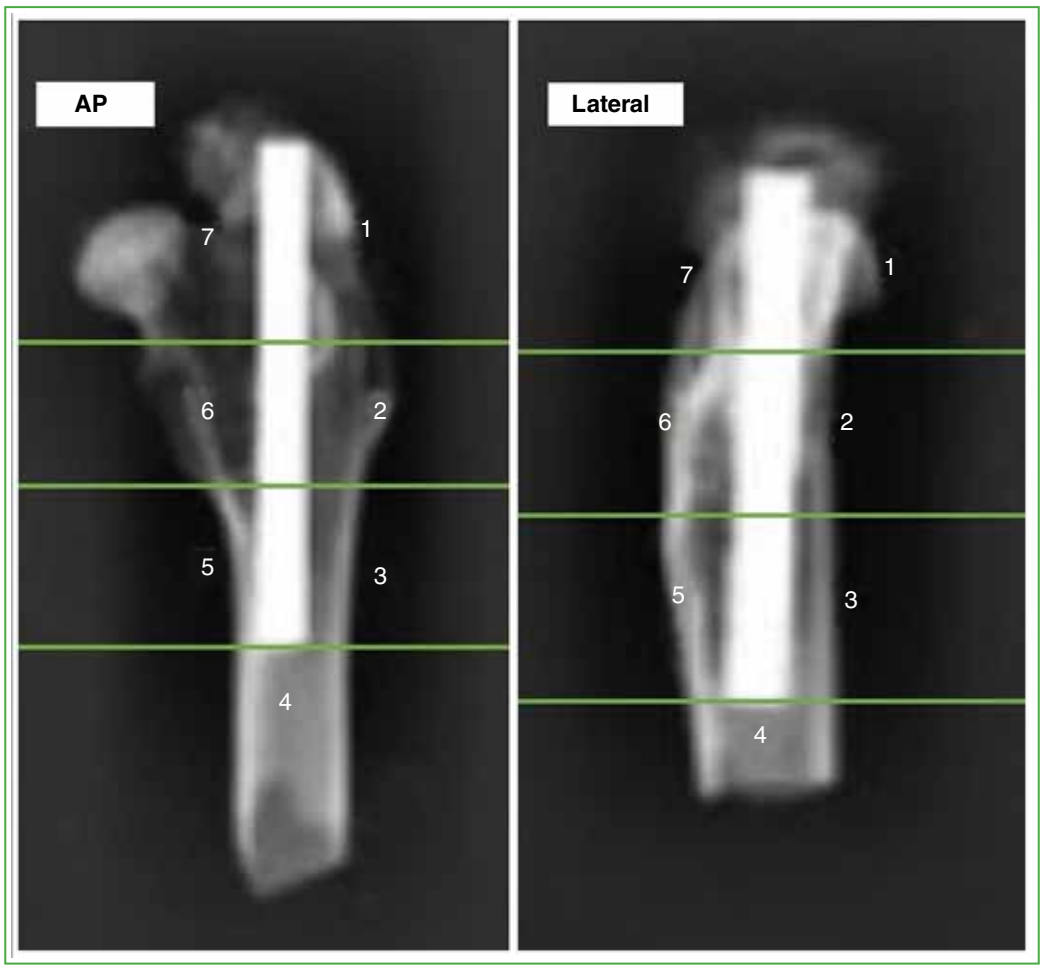

Figure 7. Division of the proximal femur according to Gruen's classification to determine the areas of union in the AP and lateral projections.

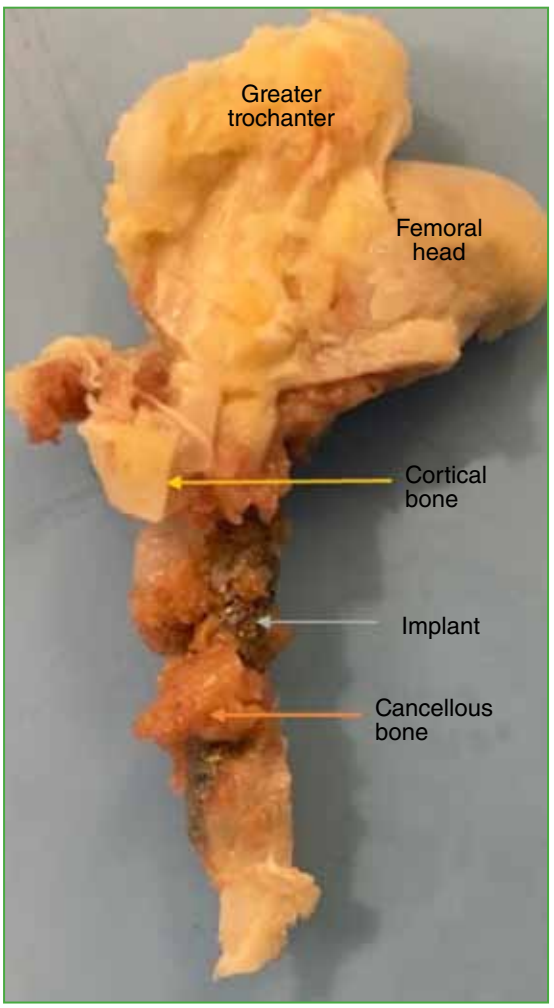

Figure 8. Cancellous bone growth around the implant.

Surgical Technique

Anesthetic induction was achieved using xylazine (5 mg/kg) and ketamine (25 mg/kg) administered intramuscularly, followed by intubation and oxygen support. Maintenance of anesthesia was provided intravenously (via the marginal ear vein) as needed, using a combination of xylazine, ketamine, and lidocaine. Continuous anesthetic monitoring and veterinary clinical oversight were maintained.

A sterile procedure was followed throughout the surgery. The operative site was shaved and disinfected. A 3 cm lateral approach was made, and the proximal femoral canal was prepared using trial rasps. The final implant diameter was selected based on the size of each rabbit's intramedullary canal. Implants were placed unilaterally, with the contralateral femur serving as a control. During the procedure, antibiotic prophylaxis was administered (cefazolin 20 mg/kg intramuscularly).

Postoperatively, the animals were inspected daily for clinical signs of complications or adverse reactions. Limb weight-bearing began from the first day of recovery, with no external support applied to the operated limb. The animals naturally adapted to weight-bearing on the operated femur, progressing to full weight-bearing.

Radiographic assessments were performed immediately postoperatively and then monthly for 12 weeks following implant placement. The treated femurs were radiographed in anteroposterior and lateral projections under anesthesia. During this period, adverse reactions or infections were also monitored.

After the last radiographic study, the animals were euthanized using an overdose of anesthesia, and the entire femur with the implant was collected for analysis. For histological examination, bone fragments were taken, after decalcification, from the areas of osseointegration observed on the radiographs.

RESULTS

No evidence of infection or other complications was detected in any of the specimens.

Clinical-Radiographic Analysis

All rabbits achieved progressive partial weight-bearing on the operated limb by the second postoperative day, without complications. By the fifth day, full weight-bearing was observed in all subjects.

No migration or subsidence was observed in any of the implants. In the anteroposterior projection, attachment points were predominantly visualized in zones 2 and 5, followed by zones 3 and 6 (Table 1).

Table 1. Radiographic location of the bone-implant junction areas. AP view.

	Zone 1	Zone 2	Zone 3	Zone 4	Zone 5	Zone 6	Zone 7
Femur 1		x			x		x
Femur 2		x			x	x	
Femur 3		x	x		x	x	
Femur 4		x	x		x		
Femur 5		x			x		
Femur 6		x	x		x	x	

The lateral projection showed junction points in zones 2, 3, and 6 (Table 2). No radiolucency or pedestal signs were detected around the implants. All femurs showed radiographic signs of osseointegration. Therefore, by 12 weeks post-surgery, adequate fixation of the implants was evident on the radiographs.

Table 2. Radiographic location of the bone-implant junction areas. Lateral view.

	Zone 1	Zone 2	Zone 3	Zone 4	Zone 5	Zone 6	Zone 7
Femur 1		x	x		x		
Femur 2		x				x	
Femur 3		x	x			x	
Femur 4		x	x			x	
Femur 5		x				x	
Femur 6		x	x			x	

The thermal arc spraying technique allowed for a more accurate recording of the areas where osseointegration occurred (Table 3). It was observed that the half of the cylinder with a roughness of 100-150 µm demonstrated greater osseointegration compared to the smoother half, which correlated with the radiographic and histological findings.

Table 3. Measurement of the maximum and minimum roughness of the implants used.

Rabbit 1		**Rabbit 2**		**Rabbit 3**	
Diameter	3.5 mm	Diameter	3.5 mm	Diameter	3.5 mm
Length	35 mm	Length	35 mm	Length	35 mm
Minimum roughness	**Maximum roughness**	**Minimum roughness**	**Maximum roughness**	**Minimum roughness**	**Maximum roughness**
11.59 µm	84.36 µm	7.35 µm	47.11 µm	4.61 µm	44.65 µm
7.19 µm	97.74 µm	6.12 µm	51.12 µm	6.94 µm	50.26 µm
8.56 µm	75.39 µm	9.58 µm	72.72 µm	9.38 µm	79.91 µm
Rabbit 4		**Rabbit 5**		**Rabbit 6**	
Diameter	3.5 mm	Diameter	3.5 mm	Diameter	3.5 mm
Length	35 mm	Length	35 mm	Length	35 mm
Minimum roughness	**Maximum roughness**	**Minimum roughness**	**Maximum roughness**	**Minimum roughness**	**Maximum roughness**
6.98 µm	83.03 µm	10.38 µm	137.84 µm	6.82 µm	78.35 µm
9.88 µm	53.47 µm	4.00 µm	42.77 µm	6.07 µm	54.39 µm
5.89 µm	59.20 µm	6.64 µm	82.32 µm	5.01 µm	56.18 µm

Histological Analysis

Histologically, all implants demonstrated newly formed bone tissue. Bone formation was particularly prominent in areas where the implant roughness ranged between 100 and 150 µm (Figure 9). In most samples, mature compact bone with concentric lamellae was clearly observed, along with areas of bone remodeling at the implant contact zone.

In regions with roughness below 100 µm, less mature bone development was noted at 12 weeks. However, areas of vascularized osteoid matrix formation were observed, indicating future bone formation and subsequent osseointegration (Figure 10). Overall, the results showed more new bone tissue in areas with roughness greater than 100 µm. The presence of established bone neoformation was demonstrated around all implants, though mechanical testing to assess the strength of bone adhesion could not be performed.

These findings suggest that increased roughness leads to greater osseointegration.

DISCUSSION

Hara et al.[15] demonstrated that porous titanium alloy implants with pore sizes of 500, 640, and 800 µm exhibit high bone ingrowth rates, which contributed to stronger bone bonding to these implants. However, the 1000 µm pore size resulted in a smaller bone area and a lower bone ingrowth rate at 12 weeks post-implantation, suggesting that a 1000 µm pore size may be too large to promote optimal bone ingrowth. Their findings suggest that the upper limit for optimal pore size is around 800 µm for porous titanium alloy implants.

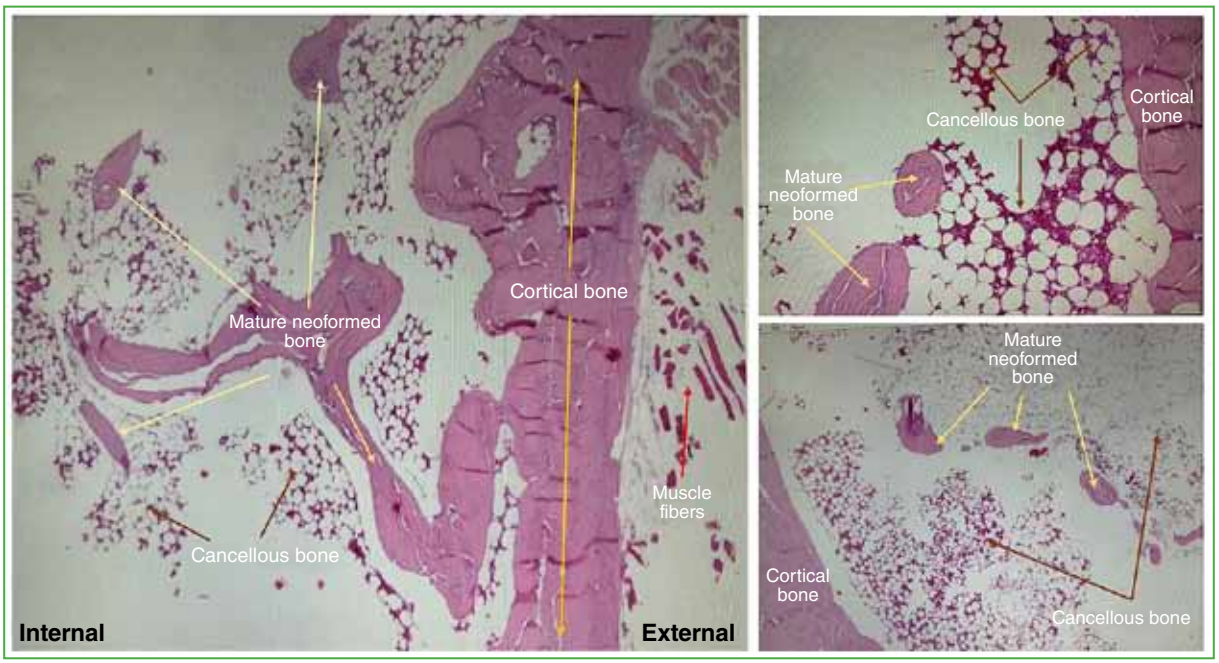

Figure 9. Histological analysis at 10x10 magnification. Mature neoformed bone is observed between the cancellous bone, which is in contact with the implant surface, indicating bone growth within the roughness.

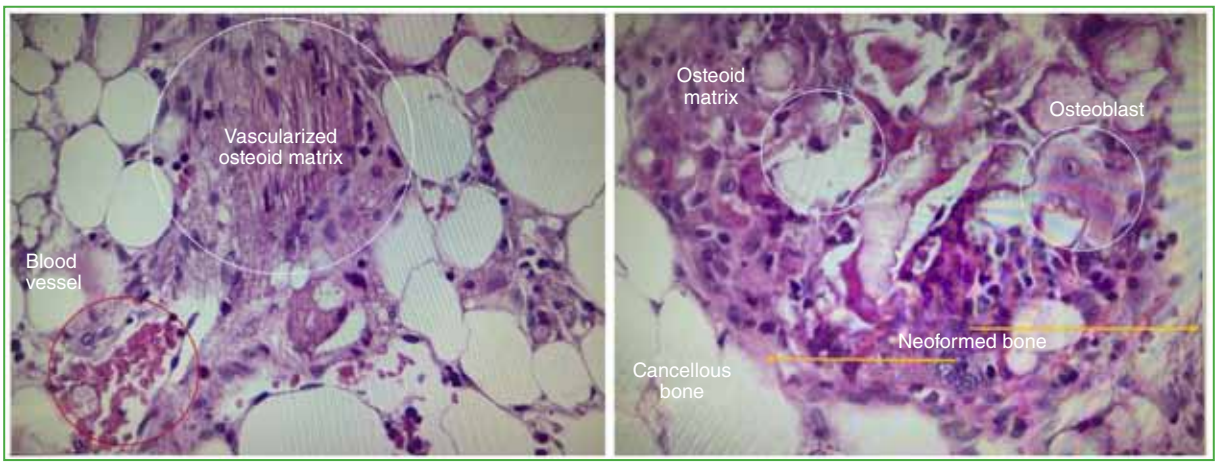

Figure 10. Histological analysis at 10x40 magnification. Tissue is visualized in a state prior to the formation of mature compact bone and osteoid matrix, osteoblasts and blood vessels.

In contrast, Hulbert et al.[16] investigated osseointegration in roughened implants generated through arc spraying and found that osteonal development requires a minimum roughness diameter between 150 and 200 µm for ceramic implants.

Similarly, several studies by Klawitter et al.[17] observed that viable osteons tend to form only when roughness sizes are between 140 and 200 µm.

Li et al.[18] reported that laser-treated surfaces require pores of at least 140 µm in diameter for osteon formation in a transcortical rabbit model.

Götz et al.[19] confirmed that bone remodeling occurs in pores with diameters of 100 µm, though with a noticeable time delay compared to larger pores. The delayed bone remodeling in 100 µm pores might compromise mechanical stability in the early weeks post-implantation, relative to implants with larger pores. Interestingly, pores of 300 µm were found to be inferior to 200 µm pores in terms of bone-to-implant contact, suggesting that larger roughness could slow osseointegration.

Our study clearly demonstrated that the greatest osseointegration occurred in areas with roughness around 100 µm. However, smaller diameter roughnesses also showed evidence of osteoid matrix formation—a precursor tissue to mature bone—which may suggest ongoing bone-implant integration, regardless of roughness size.

There are inherent limitations in the design of animal studies. As previously mentioned, the proximal femoral intramedullary implant model was developed to evaluate implant material and surface properties without the added variability of mechanical testing. Thus, this model is aimed at assessing the host's initial response to the implant and the osseointegration capacity generated upon implant contact.

The rabbits used in the study were young adults (skeletally mature), providing a bone bed that healed well due to their youth. However, the non-weight-bearing nature of the model may have introduced a favorable bias in bone ingrowth data.

Additionally, the two-dimensional assessment of bone growth rates may vary depending on section selection. A three-dimensional evaluation using computed microtomography is recommended for a more accurate assessment of bone growth. Although the small number of subjects for histological examination was a limitation, similar bone growth patterns were observed in all samples. Future studies should focus on quantifying the relationship between bone bond strength and histological bone growth.

A key strength of this study is that, to the authors' knowledge, there are no national studies in Argentina that have described the surface properties of metal produced by thermal spraying, its biological characteristics, and its osseointegration capacity in endoprostheses.

CONCLUSIONS

The surface of an implant plays a critical role in osseointegration. In this study, surfaces with roughness greater than 100 µm elicited a favorable biological response, resulting in a direct bond between the implant and bone. While this study identified osseointegration at the morphological level, future research should aim to correlate these observations with biomechanical evaluations of the implants. Expanding this research to a weight-bearing model, which would impose greater demands on the implants, would help confirm the tentative conclusions we have drawn.

Conflict of interest: Dr. Carlos A. Vega is a consultant to IMECO S. A. The the rest of the authors declare no conflicts of interest. This work was funded by IMECO S.A.

F. Moruno ORCID ID: https://orcid.org/0000-0002-9522-4079

D. Veneri ORCID ID: https://orcid.org/0009-0007-9880-8735

REFERENCES

1. Park JB. Orthopedic prosthesis fixation. *Ann Biomed Eng* 1992;20(6):583-94. https://doi.org/10.1007/BF02368607
2. Yamada H, Yoshihara Y, Henmi O, Morita M, Shiromoto Y, Kawano T, et al. Cementless total hip replacement: past, present, and future. *J Orthop Sci* 2009;14(2):228-41. https://doi.org/10.1007/s00776-008-1317-4

3. Bobyn JD, Tanzer M, Miller JE. Fundamental principles of biologic fixation. In: Morrey BF (ed). *Reconstructive surgery of the joints*. New York, NY: Churchill Livingstone; 1996, p. 75-94.
4. Svehla M, Morberg P, Zicat B, Bruce W, Sonnabend D, Walsh WR. Morphometric and mechanical evaluation of titanium implant integration: comparison of five surface structures. *J Biomed Mater Res* 2000;51(1):15-22. https://doi.org/10.1002/(sici)1097-4636(200007)51:1<15::aid-jbm3>3.0.co;2-9
5. Brånemark R, Brånemark PI, Rydevik B, Myers RR. Osseointegration in skeletal reconstruction and rehabilitation: a review. *J Rehabil Res Dev* 2001;38(2):175-81. PMID: 11392650
6. Daugaard H, Elmengaard B, Bechtold JE, Jensen T, Soballe K. The effect on bone growth enhancement of implant coatings with hydroxyapatite and collagen deposited electrochemically and by plasma spray. *J Biomed Mater Res A* 2010;92(3):913-21. https://doi.org/10.1002/jbm.a.32303
7. Bobyn JD, Stackpool GJ, Hacking SA, Tanzer M, Krygier JJ. Characteristics of bone ingrowth and interface mechanics of a new porous tantalum biomaterial. *J Bone Joint Surg Br* 1999;81(5):907-14. https://doi.org/10.1302/0301-620x.81b5.9283
8. Hench LL, Best S. Ceramics, glasses and glass-ceramics. In: Ratner BD, Hoffman AS, Schoen FJ, Lemons JE (eds). *Biomaterials science. An introduction to materials in medicine*. 2ª ed. Philadelphia: Elsevier Inc.; 2004, p.153-70.
9. Fyhrie DP, Carter DR, Schurman DJ. Effects of ingrowth, geometry, and material on stress transfer under porous-coated hip surface replacements. *J Orthop Res* 1988;6(3):425-33. https://doi.org/10.1002/jor.1100060314
10. Cooley DR, Van Dellen AF, Burgess JO, Windeler AS. The advantages of coated titanium implants prepared by radiofrequency sputtering from hydroxyapatite. *J Prosthet Dent* 1992;67(1):93-100. https://doi.org/10.1016/0022-3913(92)90057-h
11. Davies JE. Bone bonding at natural and biomaterial surfaces. *Biomaterials* 2007;28(34):5058-67. https://doi.org/10.1016/j.biomaterials.2007.07.049
12. Spector M. Bone ingrowth into porous metals. In: Williams DF (ed). *Biocompatibility of orthopaedic implants*. Florida: CRC Press; 1982, p. 89-128.
13. Haddad RJ Jr, Cook SD, Thomas KA. Biological fixation of porous-coated implants. *J Bone Joint Surg Am* 1987;69(9):1459-66. PMID: 3326881
14. Fernández J, Gilemany JM, Gaona M. La proyección térmica en la obtención de recubrimientos biocompatibles ventajas de la proyección térmica por alta velocidad (HVOF) sobre la proyección térmica por plasma atmosférico (APS). CPT Centro de Proyección Térmica. Departamento de Ingeniería Química y Metalúrgica. Universidad de Barcelona; 2005, vol. 13, p. 16-39. https://doi:10.5821/sibb.v13i1.1726
15. Hara D, Nakashima Y, Sato T, Hirata M, Kanazawa M, Kohno Y, et al. Bone bonding strength of diamond-structured porous titanium-alloy implants manufactured using the electron beam-melting technique. *Mater Sci Eng C Mater Biol Appl* 2016;59:1047-52. https://doi.org/10.1016/j.msec.2015.11.025
16. Hulbert SF, Cooke FW, Klawitter JJ, Leonard RB, Sauer BW, Moyle DD, et al. Attachment of prostheses to the musculoskeletal system by tissue ingrowth and mechanical interlocking. *J Biomed Mater Res* 1973;7(3):1-23. https://doi.org/10.1002/jbm.820070303
17. Klawitter JJ, Weinstein AM. The status of porous materials to obtain direct skeletal attachment by tissue ingrowth. *Acta Orthop Belg* 1974;40:755-65. PMID: 4469737
18. Li J, Liao H, Fartash B, Hermansson L, Johnsson T. Surface-dimpled commercially pure titanium implant and bone ingrowth. *Biomaterials* 1997;18(9):691-6. https://doi.org/10.1016/s0142-9612(96)00185-8
19. Götz HE, Müller M, Emmel A, Holzwarth U, Erben RG, Stangl R. Effect of surface finish on the osseointegration of laser-treated titanium alloy implants. *Biomaterials* 2004;25:4057-64. https://doi:10.1016/j.biomaterials.2003.11.002